Received: 7 March 2024 | Revised: 17 July 2024 | Accepted: 20 August 2024

DOI: 10.1002/bit.28833

ARTICLE

BIOTECHNOLOGY AND BIOENGINEERING WILEY

Insights into yeast response to chemotherapeutic agent through time series genome-scale metabolic models

Muhammed E. Karabekmez

Department of Bioengineering, Istanbul Medeniyet University, Istanbul, Turkey

Correspondence
Muhammed E. Karabekmez, Department of Bioengineering, Istanbul Medeniyet University, Istanbul, Turkey.
Email: erkan.karabekmez@medeniyet.edu.tr

Abstract

Organism-specific genome-scale metabolic models (GSMMs) can unveil molecular mechanisms within cells and are commonly used in diverse applications, from synthetic biology, biotechnology, and systems biology to metabolic engineering. There are limited studies incorporating time-series transcriptomics in GSMM simulations. Yeast is an easy-to-manipulate model organism for tumor research. Here, a novel approach (TS-GSMM) was proposed to integrate time-series transcriptomics with GSMMs to narrow down the feasible solution space of all possible flux distributions and attain time-series flux samples. The flux samples were clustered using machine learning techniques, and the clusters' functional analysis was performed using reaction set enrichment analysis. A time series transcriptomics response of Yeast cells to a chemotherapeutic reagent—doxorubicin—was mapped onto a Yeast GSMM. Eleven flux clusters were obtained with our approach, and pathway dynamics were displayed. Induction of fluxes related to bicarbonate formation and transport, ergosterol and spermidine transport, and ATP production were captured. Integrating time-series transcriptomics data with GSMMs is a promising approach to reveal pathway dynamics without any kinetic modeling and detects pathways that cannot be identified through transcriptomics-only analysis. The codes are available at https://github.com/karabekmez/TS-GSMM.

KEYWORDS

doxorubicin, genome scale metabolic models, time series transcriptomics, yeast

1 | INTRODUCTION

Dynamics of metabolic pathways can be elucidated by different methods. Kinetic modeling is the most plausible approach at first sight but the excessive number of kinetic constants brought complications for this type of approach. To reduce complexity, some efforts focus on simplifying genome scale metabolic models (GSMM) to enable targeted kinetic models (van Rosmalen et al., 2021). GSMMs, firstly used to estimate flux distributions in steady state (FBA: Flux Balance Analysis; pFBA: Parsimonious FBA) (Lewis et al., 2010; Mishra et al., 2016; Orth et al., 2010) and to predict pseudo dynamic flux behaviors (dFBA: Dynamic FBA) (Mahadevan et al., 2002; Scott et al., 2023; Shene et al., 2020). Integrative analysis of transcriptomics and GSMMs is also common especially in higher organisms to make use of tissue or cell type specific GSMMs (Huang & Yoon, 2020a; Wang et al., 2012). In some studies, conventional metabolic flux analysis is used by adding dynamic metabolomics (Goel et al., 2008; Sriyudthsak et al., 2016) or dynamic transcriptomics (Bezjak et al., 2021) into the picture. Dynamic metabolomics can also integrated with GSMMs by manipulating constraints (uFBA) (Bordbar

et al., 2017) or objective function (Metab_FBA) (Hastings et al., 2019) considering each time point separately, however time-series metabolomic data set are rare. The study by Hastings et al., builds time point specific GSMMs by using time-series transcriptomics towards E-Flux method (Colijn et al., 2009) before using dynamic metabolomics in the objective function (Hastings et al., 2019). In another recent study, time point specific GSMMs were constructed by using GIMME approach (Becker & Palsson, 2008) by integrating dynamic transcriptomics and then FBA was utilized to simulate growth characteristics (Huang & Yoon, 2020b). However, GIMME approach yields almost the same network for each time step and flux variability should also be accounted. E-Flux sounds more plausible approach as it only manipulates flux bounds instead of eliminating reactions from the network. However, focusing on single flux distribution either by FBA or Metab_FBA might miss the flux variability within a single time point. Additionally, in many cases cells grow sub-optimally, especially in stress conditions results of FBA should be handled cautiously and alternative objective functions should be employed (Metris et al., 2012). Sampling the whole feasible solution space without searching for any optimality is another common approach in GSMM-related flux analysis (Bernstein et al., 2021). Such a Bayesian inference is promising if the solution space is narrowed down by integrating omics data (Ramon et al., 2018). There are multiple algorithms for sampling the solution space; the artificially centered hit-and-run (ACHR) algorithm (Kaufman & Smith, 1998) and the coordinate hit-and-run with rounding (CHRR) algorithms (Haraldsdóttir et al., 2017) are sampling around optimal biomass production while Bayesian FBA (bFBA) (Heinonen et al., 2019) relaxes growth optimality to sample with a higher variance. The most important challenge in sampling is unreasonable run times for large GSMMs (Fallahi et al., 2020).

In this study, a pipeline called Time Series Genome Scale Metabolic Modeling (TS-GSMM) was proposed. Firstly, a modified version of E-Flux, fE-Flux (Karabekmez, 2023), which guarantees feasibility of the resulting models, was employed to construct time step-specific constrained GSMMs from a Yeast GSMM by integrating a time series transcriptomic data set collected after exposure to doxorubicin in a chemostat environment. ACHR approach was used to sample the flux cone for each time point, and the Wasserstein distance was used to create a distance matrix of time points for each reaction. The normalized distances of the resulting matrices were clustered using a k-medoid clustering approach. The obtained pseudo-dynamic flux clusters were functionally annotated through reaction set enrichment analysis.

2 | MATERIALS AND METHODS

A recent and moderate size GSMM for yeast, namely Yeast6 (Heavner et al., 2013) was retrieved. Yeast6, v6.0.0 has 1882 reactions, 1454 metabolites and 901 genes out of which 881 metabolic genes' expression values present in the transcriptomic data set. The transcriptomic data set consists of a time series response of yeast cells to a common therapeutic agent, doxorubicin in a chemostat (Karabekmez et al., 2021). The data set can be reached from Array Express by accession number E-MTAB-10023.

The steps for TS-GSMM were conducted by using Cobra Toolbox (v.3.0) (Heirendt et al., 2019) in Matlab. Reaction boundaries in the Yeast6 model were adjusted by using Flux Variability Analysis (FVA) (Mahadevan & Schilling, 2003) letting 80% of the optimal objective function—biomass production possible, to be able to simulate sub-optimality under stress conditions. In the literature, mostly 90% of the optimal growth rate was assumed to address sub-optimality (Wintermute et al., 2013), however in TS-GSMM approach is not using solely the results of FVA, instead it uses sampling method to span the feasible solution space. Therefore, 80% was arbitrarily chosen to span even further solution space to the optimal flux distributions. For each time point of the time-series transcriptomic data set, reaction expressions were calculated by using GPR rules and metabolic gene expression values. *mapExpressionToReactions* function in the Cobra Toolbox was used for this purpose. This function takes gene expression values for each metabolic gene and a GSMM as inputs and calculates reaction expression values.

As proposed in E-Flux approach (Colijn et al., 2009) adjusted reaction boundaries in the Yeast6 model were narrowed down proportional to the ratio of normalized reaction expression values to the highest expression level in the GSMM of the same time point. However, these reaction boundary manipulations may lead to an infeasible GSMM. To prevent infeasibility, fE-Flux which is a modified version of E-Flux was implemented. fE-Flux skips reaction bound manipulations that leads to an infeasible model by checking model feasibility one by one after each boundary manipulation and returns to the original boundary values for the reactions that boundary alteration causes infeasibility (Karabekmez, 2023).

The artificially centered hit-and-run (ACHR) algorithm (Kaufman & Smith, 1998) was applied to span feasible solution space within time point specific GSMMs by using *sampleCbModel* function in the Cobra Toolbox. 2000 flux points were sampled for each reaction within each GSMM.

Pairwise distances of sampling distributions between time points were calculated by 1-Wasserstein distance (Kolbe, 2023) in Matlab. p-norm distance between generated distance matrices for each time series couple was assigned as flux profile distances. k-medoid clustering was used to get flux clusters out of it.

To decide the number of clusters for k-medoid clustering, Calinski-Harabasz clustering evaluation criterion (CH index) (Calinski & Harabasz, 1974) and silhouette scores were calculated by using *evalclusters* function in Matlab R2022a (MATLAB, 2022). To measure partitioning power of the number of clusters sum of squares of number of fluxes in each resulting cluster were also calculated.

Reaction set enrichment analysis were conducted by using KEGG (Kanehisa, 2000) reaction networks for Yeast. Hypergeometric distribution was used to calculate p-values and Bonferroni correction was used to avoid multiple testing problems. 0.05 was used as threshold for corrected p-values.

Yeast metabolic pathway plots were retrieved from KEGG (Kanehisa, 2000). Box plots of flux samplings were obtained in Matlab R2022a.

TABLE 1 The Numbers of fluxes in each cluster found by k-medoid approach.

Cluster ID	1	2	3	4	5	6	7	8	9	10	11
Number of Fluxes in the cluster	884	16	6	8	12	1	3	16	9	1	9

3 | RESULTS

Yeast GSMM v6.0.0 has 1882 reactions, 1454 metabolites and 901 genes, out of which 881 metabolic genes' expression values are present in the transcriptomic data set. In conventional E-Flux applications the transcriptomics mapped GSMMs can be infeasible. In this study, all initially constructed time point specific GSMMs were found to be infeasible, that is no growth could be simulated. Therefore, we have used the fE-flux method. Initially FVA was applied by tolerating up to 80% of the optimal growth to find minimum and maximum flux boundaries (minFlux and maxFlux) for all fluxes in the reference Yeast6 GSMM.

Then minFLux—maxFlux interval for each reaction in each time point was narrowed down proportional to the ratio of the corresponding reaction expression to the maximum reaction level for that time point. The reactions leading infeasibility were skipped.

It was observed that for 12 time point specific GSMMs that were constructed, upper bound adjustments of 8 to 10 reactions' upper bound modifications led to infeasibility, out of which 8 reactions were the same for all time points. It means lowering those sensitive reactions' upper bounds causes infeasibility. When we investigated the minFlux—maxFlux interval for those reactions and observed that typically all have a very narrow interval. The difference between the upper and lower bounds for these reactions are between 289E-5 and 126E-4, while 90% of the non-zero flux intervals are larger than this. ACHR sampling procedure was reduced time point specific GSMMs into models of identical reaction and metabolite sets of 965 reactions and 704 metabolites for 10 time points. For the first two time points, there were 10 additional reactions which were excluded from the rest of the study. Pairwise distances of sampling distributions among 12 time points were calculated for 965 reactions by 1-Wasserstein distance for each time point. Unlike Kullback–Leibler divergence (Fass, 2023) or Kolmogorov–Smirnov statistic (Massey, 1951), Wasserstein distance gives an idea about true distance (Muskulus & Verduyn-Lunel, 2011). The distance matrix was clustered by k-medoids clustering approach assigning 11 as number of clusters which yields the highest number of clusters with seven or more fluxes as CH-index or silhouette scores were not helpful to decide the optimal number of clusters. The resulting numbers of fluxes in the clusters (Table 1) shows that majority of the fluxes resides in the same cluster (cluster 1) where there was no characteristic time series trend.

KEGG ID's corresponding to reactions in the GSMM were already provided in Yeast6 but not all reactions have matches in KEGG like transport and exchange reactions. The clusters in which less than 3 KEGG ID's are assigned were not used for reaction set enrichment analysis. Cluster 1, 2, 4, and 9 have more than 3 reactions with KEGG ID. Nucleotide and amino acid metabolism

TABLE 2 The number of fluxes in each cluster found by k-medoid approach.

KEGG pathway	Corrected p-values	Number of reactions	Number of matches
CLUSTER 1			
Pyrimidine metabolism	000E + 00	100	32
Purine metabolism	000E + 00	154	45
Cysteine and methionine metabolism	398E-10	100	22
Alanine aspartate and glutamate metabolism	329E-09	47	15
Valine leucine and isoleucine biosynthesis	236E-08	25	11
Pyruvate metabolism	453E-08	83	18
Phenylalanine tyrosine and tryptophan biosynthesis	568E-08	48	14
One carbon pool by folate	113E-06	34	11
Glycine serine and threonine metabolism	395E-06	75	15
Carbon fixation in photosynthetic organisms	165E-04	26	8
Pantothenate and CoA biosynthesis	204E-04	35	9
Carbon fixation pathways in prokaryotes	287E-04	56	11
Citrate cycle (TCA cycle)	322E-03	28	7
Lysine biosynthesis	430E-03	39	8
Arginine biosynthesis	650E-03	31	7
Glycolysis/ Gluconeogenesis	128E-02	57	9
Glycerophospholipid metabolism	353E-02	93	11
Histidine metabolism	397E-02	53	8
Steroid biosynthesis	443E-02	67	9
Fatty acid biosynthesis	494E-02	68	9
CLUSTER 2			
Carbon fixation in photosynthetic organisms	621E-04	26	2
Pyruvate metabolism	644E-03	83	2
CLUSTER 4			
Galactose metabolism	225E-06	58	3
Amino sugar and nucleotide sugar metabolism	386E-05	148	3
CLUSTER 9			
Phenylalanine tyrosine and tryptophan biosynthesis	253E-04	48	2

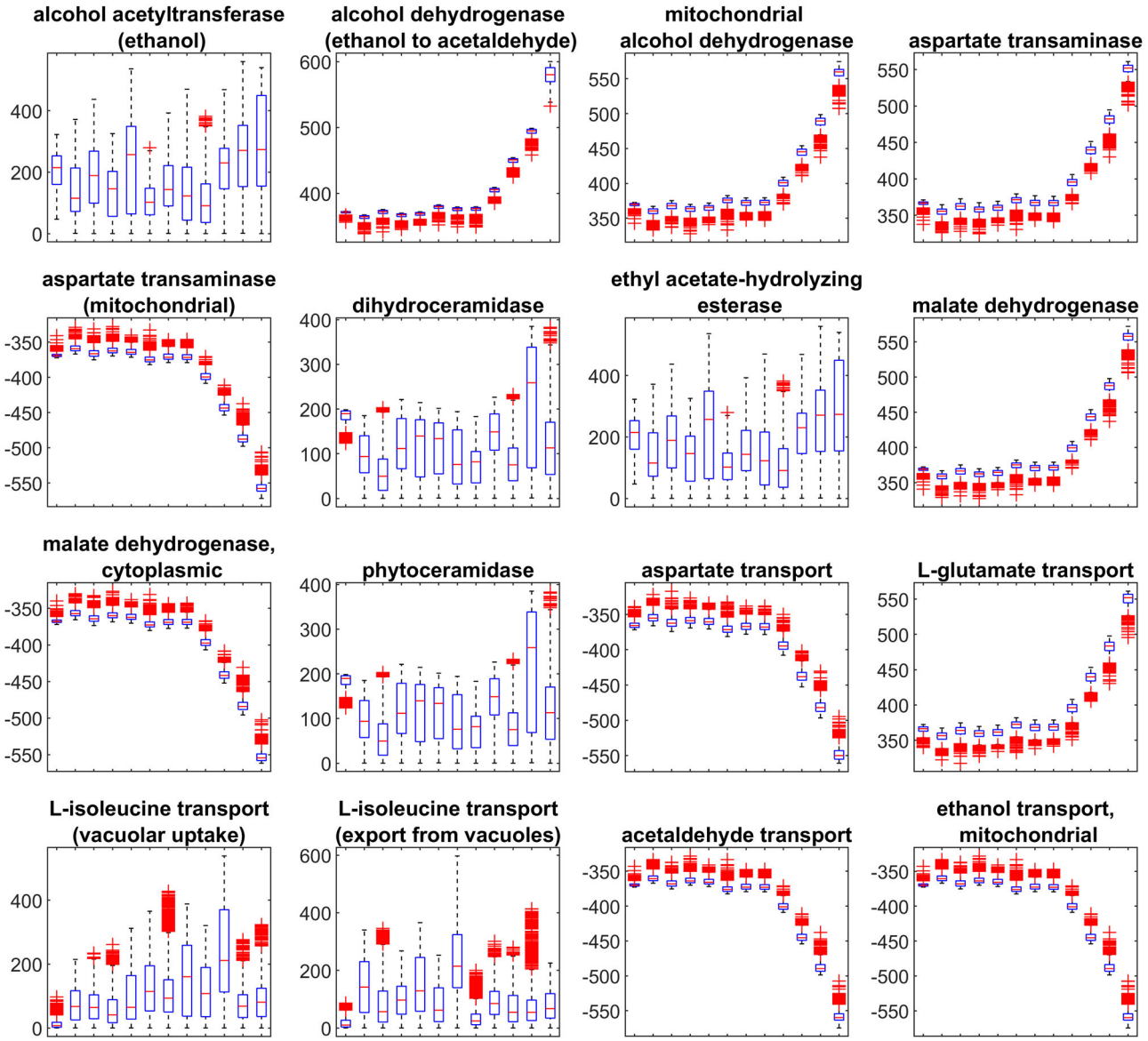

FIGURE 1 Flux sampling profiles in cluster 2. Each box plot represents flux sampling distribution at a time point.

related pathways were found to be enriched in cluster 1. The second cluster was found to be enriched in pyruvate metabolism and galactose metabolism is linked to cluster 4. The pathway for biosynthesis of aromatic amino acids, phenylalanine tyrosine and tryptophan, was observed to be significantly associated with both cluster 1 and cluster 9 (Table 2).

Energy metabolism related fluxes are enriched in the cluster 2. Transport fluxes of malate-aspartate NADH shuttle were augmented in long term response. Ethanol processing and transport in mitochondria was also observed to be enhanced in a correlated trend (Figure 1).

All reactions in cluster 3 are related to bicarbonate formation (in cytoplasm and nucleus) and transport of carbon dioxide and water between nucleus and cytoplasm related to the bicarbonate formation reactions. Flux profiles shows that bicarbonate formation is shifted from nucleus to cytoplasm and there are two consecutive shifts in the reaction directions. After the changes in the reaction direction the initial state is reattained in the long term (Supporting Information S1: Figure S1).

There are 4 enzymatic reactions and 4 transport reactions in cluster 4. The enzymatic reactions are related to galactose metabolism (Table 2) while the rest are L-leucine and fatty acid transport associated transport reactions. Initial (before the pulse) flux distributions of these transport reactions are closer to zero and they tend to increase after the introduction of the chemotherapeutic (Supporting Information S1: Figure S2).

Ergosterol, spermidine and glycerol transport related fluxes reside in cluster 5. All these reactions seem to be induced upon introduction of doxorubicin into the chemostat environment (Supporting Information S1: Figure S3). Similar to cluster 3 and cluster 5, cluster 8 and cluster 11 were also found to be occupied dominantly by transport reactions. Increase in fluxes of AMP/ATP transporter, transport of ATP and some amino acids were indicated in the cluster 8 (Supporting

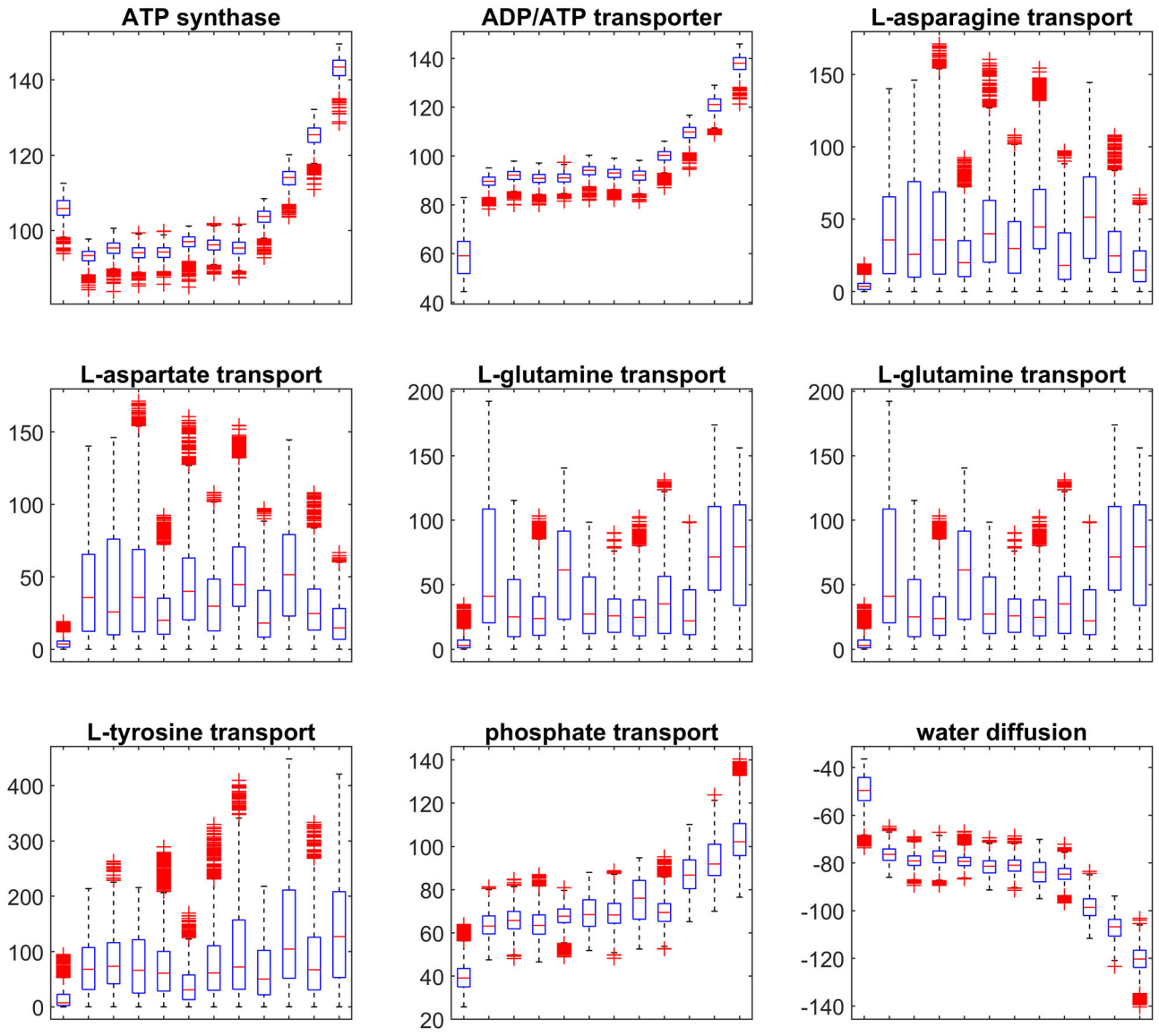

FIGURE 2 Flux sampling profiles in cluster 11. Each box plot represents flux sampling distribution at a time point.

Information S1: Figure S4). ATP synthase, ADP/ATP transporter, water diffusion and phosphate trans-port fluxes were observed to be induced in long term with a trend of flux distributions with much lower variances in the cluster 11. ATP synthase flux drops immediately after the pulse but increases in long term (Figure 2).

Growth and glucose transport profiles are quite similar with a small initial increase and subsequent relatively higher decrease. Note that the difference between the top and bottom points is quite small though significant (Figure 3).

When glycolysis pathway investigated in detail, it was observed that fluxes of four consecutive reactions from cluster 1; phosphoglycerate kinase, phosphoglycerate mutase, enolase and pyruvate kinase were sampled. Mean of flux values of phosphoglycerate kinase tend to decrease and that of pyruvate kinase tend to increase. The two reactions in between show no significant flux sampling distribution. It is interesting that reaction expression profiles give no clue for flux sampling profiles (Figure 4).

4 | DISCUSSION

Malate-aspartate NADH shuttle (MAS) in yeast was reported to be one of the important mediators of extending life span (Easlon et al., 2008). It was also shown that aerobic glycolysis, which is one of the characteristic of tumor cells, can be limited by inducing MAS (Wang et al., 2022). It is displayed in this study that MAS related transport fluxes were upregulated (Figure 1) upon exposure to doxorubicin. Interestingly this could help to build new hypotheses for lightening the mechanisms of antitumor activity of doxorubicin. Insufficiency of MAS could be related to heart failure (Lee et al., 2016) which is the most common side effect of doxorubicin. It is already reported that drugs inhibiting MAS can prevent cardiotoxicity of doxorubicin (Liu et al., 2014). ATP production is also an important issue in cardio toxic side effect of doxorubicin. In human heart it is known that doxorubicin reduces ATP production efficiency (Li et al., 2022). Short term response of yeast cells might be

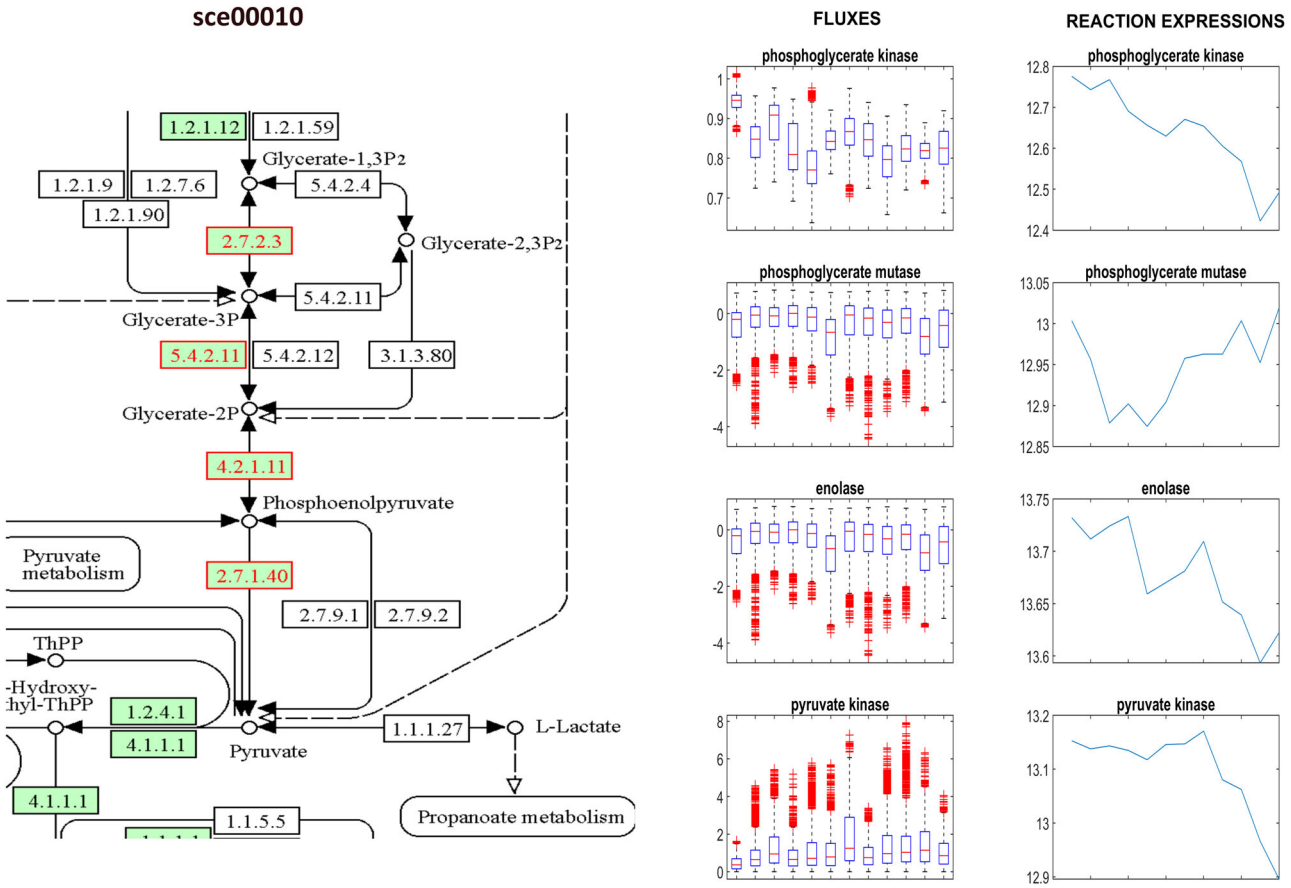

FIGURE 3 Flux sampling profiles of growth reaction (left) and glucose transport (right). x-axis is nonuniform time points in minutes.

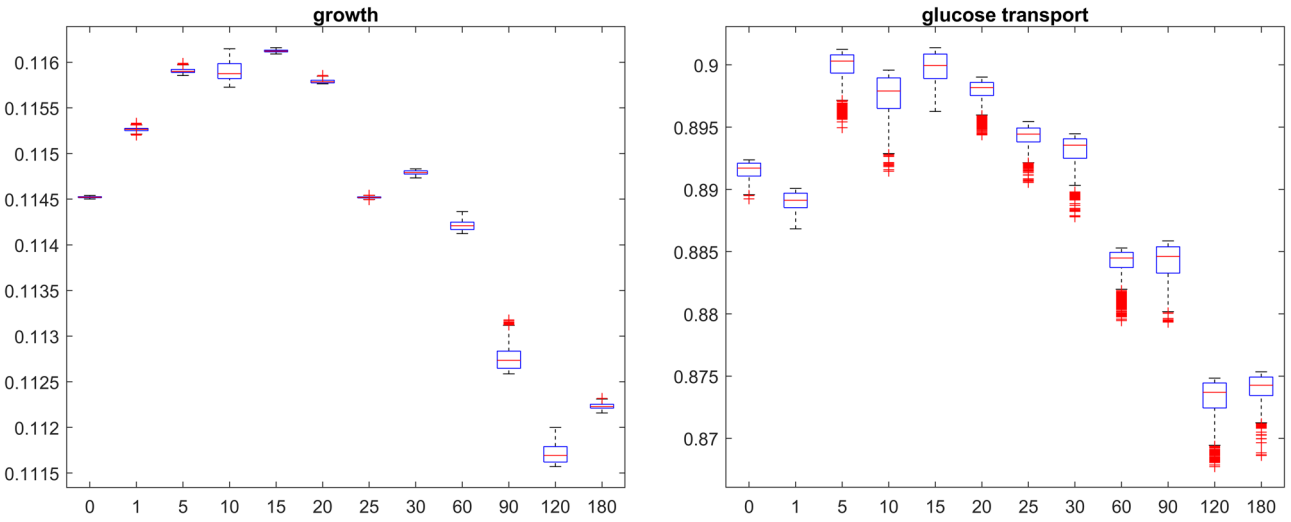

FIGURE 4 Flux sampling profiles of reactions glycolysis pathway. (sce00010: partial KEGG glycolysis pathway for yeast; FLUXES: flux sampling profiles for the reactions highlighted in red in the KEGG network with the same order. Each box plot represents flux sampling distribution at a time point; REACTION EXPRESSIONS: Reaction expressions obtained by mapping gene expressions to the GSMM by GPR rules).

simulating this phenomenon (Figure 2). In long term, yeast cells activate MAS and increases ATP production and related transport reactions.

In cluster 3, flux sampling profiles points a shift in directions of bicarbonate formation reactions resulting in down regulation of nucleolar bicarbonate formation and a reverse effect in the cytoplasm (Figure S1). Bicarbonate formation has important roles in human diseases through its role in pH buffering (Alka & Casey, 2014). It is also suggested that tumor cells may induce bicarbonate transport to regulate pH and resist to chemotherapeutics (McIntyre et al., 2016).

Bicarbonate's possible role in cardiotoxicity of doxorubicin was also discussed in the literature (Konorev et al., 2000).

Spermidine is claimed to induce autophagy of organelles to increase lifespan of yeast (Madeo et al., 2010). It can be hypothesized that doxorubicin leads to damages inside cells through formation of reactive oxygen species and yeast cells induce spermidine flux in response to this stress. Ergosterol plays a similar role in yeast with cholesterol's role in human; it's essential for membrane formation and maintenance. It is known that Ergosterol transport is enhanced in tumor cells to promote growth. Here, in this context a possible explanation is that—similar to cholesterol—yeast cells might be trying to reduce cellular doxorubicin concentration through ergosterol (Alves et al., 2017; Yamauchi & Rogers, 2018). In this study, the flux changes detected in the cluster 5 captures induction in reactions related to ergosterol and spermidine transport (Supporting Information S1: Figure S3). Metabolomic studies investigating the effects of doxorubicin on yeast cells have revealed that inositol concentration increases upon exposure to doxorubicin (Heux et al., 2012) which supports these findings that it triggers stress responsive lipid pathways.

GSMM provides a template to reflect flux dynamics without involving reaction kinetics by integrating time series transcriptomics datasets. Time series transcriptomic data analysis without GSMMs cannot capture metabolic dynamics and before TS-GSMM there were no well-defined approach to incorporate GSMMs. The proposed method captures metabolic pathways that cannot unveiled by analyzing solely the original transcriptomic data (Karabekmez et al., 2021; Taymaz-Nikerel et al., 2018). Time series transcriptomic datasets are not as common as conventional transcriptomic studies. The first GSMMs in the literature were constructed for unicellular organisms. Therefore, a time series transcriptomic data set collected after a chemotherapeutic pulse was chosen as case study to investigate in silico fluxomics dynamics. The approach has been shown to have a potential to be extended to higher organisms and more complicated cases. Future studies on time series proteomics can improve the performance of the proposed method.

ACKNOWLEDGMENTS

The author kindly express his gratitude to Prof. Dr. Mehmet Güray Güler, Furkan Cantürk and Merve Yarıcı for helpful discussions on technical details.

CONFLICT OF INTEREST STATEMENT

The author declares no conflict of interest.

DATA AVAILABILITY STATEMENT

The codes for TS-GSMM and simulations were deposited at https://github.com/karabekmez/TS-GSMM.

ORCID

Muhammed E. Karabekmez https://orcid.org/0000-0002-0517-5227

REFERENCES

Alka, K., & Casey, J. R. (2014). Bicarbonate transport in health and disease. *IUBMB Life*, *66*, 596–615. https://doi.org/10.1002/iub.1315

Alves, A. C., Magarkar, A., Horta, M., Lima, J. L. F. C., Bunker, A., Nunes, C., & Reis, S. (2017). Influence of doxorubicin on model cell membrane properties: Insights from in vitro and in silico studies. *Scientific Reports*, *7*, 6343. https://doi.org/10.1038/s41598-017-06445-z

Becker, S. A., & Palsson, B. O. (2008). Context-specific metabolic networks are consistent with experiments. *PLoS Computational Biology*, *4*, e1000082. https://doi.org/10.1371/journal.pcbi.1000082

Bernstein, D. B., Sulheim, S., Almaas, E., & Segrè, D. (2021). Addressing uncertainty in genome-scale metabolic model reconstruction and analysis. *Genome Biology*, *22*, 64. https://doi.org/10.1186/s13059-021-02289-z

Bezjak, L., Erklavec Zajec, V., Baebler, Š., Stare, T., Gruden, K., Pohar, A., Novak, U., & Likozar, B. (2021). Incorporating RNA-Seq transcriptomics into glycosylation-integrating metabolic network modelling kinetics: Multiomic Chinese hamster ovary (CHO) cell bioreactors. *Biotechnology and Bioengineering*, *118*, 1476–1490. https://doi.org/10.1002/bit.27660

Bordbar, A., Yurkovich, J. T., Paglia, G., Rolfsson, O., Sigurjónsson, Ó. E., & Palsson, B. O. (2017). Elucidating dynamic metabolic physiology through network integration of quantitative time-course metabolomics. *Scientific Reports*, *7*, 46249. https://doi.org/10.1038/srep46249

Calinski, T., & Harabasz, J. (1974). A dendrite method for cluster analysis. *Communications in Statistics-Theory and Methods*, *3*, 1–27. https://doi.org/10.1080/03610927408827101

Colijn, C., Brandes, A., Zucker, J., Lun, D. S., Weiner, B., Farhat, M. R., Cheng, T.-Y., Moody, D. B., Murray, M., & Galagan, J. E. (2009). Interpreting expression data with metabolic flux models: Predicting mycobacterium tuberculosis mycolic acid production. *PLoS Computational Biology*, *5*, e1000489. https://doi.org/10.1371/journal.pcbi.1000489

Easlon, E., Tsang, F., Skinner, C., Wang, C., & Lin, S.-J. (2008). The malate-aspartate NADH shuttle components are novel metabolic longevity regulators required for calorie restriction-mediated life span extension in yeast. *Genes & Development*, *22*, 931–944. https://doi.org/10.1101/gad.1648308

Fallahi, S., Skaug, H. J., & Alendal, G. (2020). A comparison of Monte Carlo sampling methods for metabolic network models. *PLoS One*, *15*, e0235393. https://doi.org/10.1371/journal.pone.0235393

Fass, D., Kullback–Leibler divergence, 2023. https://www.mathworks.com/matlabcentral/fileexchange/13089-kldiv (accessed 6 August 2023).

Goel, G., Chou, I.-C., & Voit, E. O. (2008). System estimation from metabolic time-series data. *Bioinformatics*, *24*, 2505–2511. https://doi.org/10.1093/bioinformatics/btn470

Haraldsdóttir, H. S., Cousins, B., Thiele, I., Fleming, R. M. T., & Vempala, S. (2017). CHRR: Coordinate hit-and-run with rounding for uniform sampling of constraint-based models. *Bioinformatics*, *33*, 1741–1743. https://doi.org/10.1093/bioinformatics/btx052

Hastings, J., Mains, A., Virk, B., Rodriguez, N., Murdoch, S., Pearce, J., Bergmann, S., Le Novère, N., & Casanueva, O. (2019). Multi-omics and genome-scale modeling reveal a metabolic shift during C. Elegans aging. *Frontiers in Molecular Biosciences*, *6*, 2. https://doi.org/10.3389/fmolb.2019.00002

Heavner, B. D., Smallbone, K., Price, N. D., & Walker, L. P. (2013). Version 6 of the consensus yeast metabolic network refines biochemical coverage and improves model performance. *Database*, *2013*, bat059. https://doi.org/10.1093/database/bat059

Heinonen, M., Osmala, M., Mannerström, H., Wallenius, J., Kaski, S., Rousu, J., & Lähdesmäki, H. (2019). Bayesian metabolic flux analysis reveals intracellular flux couplings. *Bioinformatics*, *35*, i548–i557. https://doi.org/10.1093/bioinformatics/btz315

Heirendt, L., Arreckx, S., Pfau, T., Mendoza, S. N., Richelle, A., Heinken, A., Haraldsdóttir, H. S., Wachowiak, J., Keating, S. M., Vlasov, V.,

Magnusdóttir, S., Ng, C. Y., Preciat, G., Žagare, A., Chan, S. H. J., Aurich, M. K., Clancy, C. M., Modamio, J., Sauls, J. T., … Fleming, R. M. T. (2019). Creation and analysis of biochemical constraint-based models using the COBRA toolbox v.3.0. *Nature Protocols*, *14*, 639–702. https://doi.org/10.1038/s41596-018-0098-2

Heux, S., Fuchs, T. J., Buhmann, J., Zamboni, N., & Sauer, U. (2012). A high-throughput metabolomics method to predict high concentration cytotoxicity of drugs from low concentration profiles. *Metabolomics*, *8*, 433–443. https://doi.org/10.1007/s11306-011-0386-0

Huang, Z., & Yoon, S. (2020a). Identifying metabolic features and engineering targets for productivity improvement in CHO cells by integrated transcriptomics and genome-scale metabolic model. *Biochemical Engineering Journal*, *159*, 107624. https://doi.org/10.1016/j.bej.2020.107624

Huang, Z., & Yoon, S. (2020b). Integration of time-series transcriptomic data with genome-scale CHO metabolic models for mAB engineering. *Processes*, *8*, 331. https://doi.org/10.3390/pr8030331

Kanehisa, M. (2000). KEGG: Kyoto encyclopedia of genes and genomes. *Nucleic Acids Research*, *28*, 27–30. https://doi.org/10.1093/nar/28.1.27

Karabekmez, M. E. (2023). fE-Flux: Feasible Flux Boundary Modification Framework for Constraint Based Metabolic Models. in: ICEANS.

Karabekmez, M. E., Taymaz-Nikerel, H., Eraslan, S., & Kirdar, B. (2021). Time-dependent re-organization of biological processes by the analysis of the dynamic transcriptional response of yeast cells to doxorubicin. *Molecular Omics*, *17*, 572–582. https://doi.org/10.1039/D1MO00046B

Kaufman, D. E., & Smith, R. L. (1998). Direction choice for accelerated convergence in hit-and-run sampling. *Operations Research*, *46*, 84–95. https://doi.org/10.1287/opre.46.1.84

Kolbe, N. (2023). Wasserstein distance, (accessed 5 August 2023). https://github.com/nklb/wasserstein-distance

Konorev, E. A., Zhang, H., Joseph, J., Kennedy, M. C., & Kalyanaraman, B. (2000). Bicarbonate exacerbates oxidative injury induced by anti-tumor antibiotic doxorubicin in cardiomyocytes. *American Journal of Physiology-Heart and Circulatory Physiology*, *279*, H2424–H2430. https://doi.org/10.1152/ajpheart.2000.279.5.H2424

Lee, C. F., Chavez, J. D., Garcia-Menendez, L., Choi, Y., Roe, N. D., Chiao, Y. A., Edgar, J. S., Goo, Y. A., Goodlett, D. R., Bruce, J. E., & Tian, R. (2016). Normalization of NAD+ redox balance as a therapy for heart failure. *Circulation*, *134*, 883–894. https://doi.org/10.1161/CIRCULATIONAHA.116.022495

Lewis, N. E., Hixson, K. K., Conrad, T. M., Lerman, J. A., Charusanti, P., Polpitiya, A. D., Adkins, J. N., Schramm, G., Purvine, S. O., Lopez-Ferrer, D., Weitz, K. K., Eils, R., König, R., Smith, R. D., & Palsson, B. Ø. (2010). Omic data from evolved *E. coli* are consistent with computed optimal growth from genome-scale models. *Molecular Systems Biology*, *6*, 390. https://doi.org/10.1038/msb.2010.47

Li, M.-J., Sun, W.-S., Yuan, Y., Zhang, Y.-K., Lu, Q., Gao, Y.-Z., Ye, T., & Xing, D.-M. (2022). Breviscapine remodels myocardial glucose and lipid metabolism by regulating serotonin to alleviate doxorubicin-induced cardiotoxicity. *Frontiers in Pharmacology*, *13*, 930835. https://doi.org/10.3389/fphar.2022.930835

Liu, Y., Asnani, A., Zou, L., Bentley, V. L., Yu, M., Wang, Y., Dellaire, G., Sarkar, K. S., Dai, M., Chen, H. H., Sosnovik, D. E., Shin, J. T., Haber, D. A., Berman, J. N., Chao, W., & Peterson, R. T. (2014). Visnagin protects against doxorubicin-induced cardiomyopathy through modulation of mitochondrial malate dehydrogenase. *Science Translational Medicine*, *6*, 266ra170. https://doi.org/10.1126/scitranslmed.3010189

Madeo, F., Eisenberg, T., Büttner, S., Ruckenstuhl, C., & Kroemer, G. (2010). Spermidine: A novel autophagy inducer and longevity elixir. *Autophagy*, *6*, 160–162. https://doi.org/10.4161/auto.6.1.10600

Mahadevan, R., Edwards, J. S., & Doyle, F. J. (2002). Dynamic flux balance analysis of diauxic growth in *Escherichia coli*. *Biophysical Journal*, *83*, 1331–1340. https://doi.org/10.1016/S0006-3495(02)73903-9

Mahadevan, R., & Schilling, C. H. (2003). The effects of alternate optimal solutions in constraint-based genome-scale metabolic models. *Metabolic Engineering*, *5*, 264–276. https://doi.org/10.1016/j.ymben.2003.09.002

Massey, F. J. (1951). The Kolmogorov–Smirnov test for goodness of fit. *Journal of the American Statistical Association*, *46*, 68–78. https://doi.org/10.1080/01621459.1951.10500769

MATLAB. (2022). *The MathWorks Inc*. MATLAB.

McIntyre, A., Hulikova, A., Ledaki, I., Snell, C., Singleton, D., Steers, G., Seden, P., Jones, D., Bridges, E., Wigfield, S., Li, J.-L., Russell, A., Swietach, P., & Harris, A. L. (2016). Disrupting hypoxia-induced bicarbonate transport acidifies tumor cells and suppresses tumor growth. *Cancer Research*, *76*, 3744–3755. https://doi.org/10.1158/0008-5472.CAN-15-1862

Metris, A., George, S., & Baranyi, J. (2012). Modelling osmotic stress by flux balance analysis at the genomic scale. *International Journal of Food Microbiology*, *152*, 123–128. https://doi.org/10.1016/j.ijfoodmicro.2011.06.016

Mishra, P., Park, G.-Y., Lakshmanan, M., Lee, H.-S., Lee, H., Chang, M. W., Ching, C. B., Ahn, J., & Lee, D.-Y. (2016). Genome-scale metabolic modeling and in silico analysis of lipid accumulating yeast *Candida tropicalis* for dicarboxylic acid production. *Biotechnology and Bioengineering*, *113*, 1993–2004. https://doi.org/10.1002/bit.25955

Muskulus, M., & Verduyn-Lunel, S. (2011). Wasserstein distances in the analysis of time series and dynamical systems. *Physica D: Nonlinear Phenomena*, *240*, 45–58. https://doi.org/10.1016/j.physd.2010.08.005

Orth, J. D., Thiele, I., & Palsson, B. Ø. (2010). What is flux balance analysis. *Nature Biotechnology*, *28*, 245–248. https://doi.org/10.1038/nbt.1614

Ramon, C., Gollub, M. G., & Stelling, J. (2018). Integrating -omics data into genome-scale metabolic network models: principles and challenges. *Essays in Biochemistry*, *62*, 563–574. https://doi.org/10.1042/EBC20180011

van Rosmalen, R. P., Smith, R. W., Martins Dos Santos, V. A. P., Fleck, C., & Suarez-Diez, M. (2021). Model reduction of genome-scale metabolic models as a basis for targeted kinetic models. *Metabolic Engineering*, *64*, 74–84. https://doi.org/10.1016/j.ymben.2021.01.008

Scott, W. T., Henriques, D., Smid, E. J., Notebaart, R. A., & Balsa-Canto, E. (2023). Dynamic genome-scale modeling of *saccharomyces cerevisiae* unravels mechanisms for ester formation during alcoholic fermentation. *Biotechnology and Bioengineering*, *120*, 1998–2012. https://doi.org/10.1002/bit.28421

Shene, C., Paredes, P., Flores, L., Leyton, A., Asenjo, J. A., & Chisti, Y. (2020). Dynamic flux balance analysis of biomass and lipid production by Antarctic thraustochytrid oblongichytrium sp. RT2316-13. *Biotechnology and Bioengineering*, *117*, 3006–3017. https://doi.org/10.1002/bit.27463

Sriyudthsak, K., Shiraishi, F., & Hirai, M. Y. (2016). Mathematical modeling and dynamic simulation of metabolic reaction systems using metabolome time series data. *Frontiers in Molecular Biosciences*, *3*, 15. https://doi.org/10.3389/fmolb.2016.00015

Taymaz-Nikerel, H., Karabekmez, M. E., Eraslan, S., & Kırdar, B. (2018). Doxorubicin induces an extensive transcriptional and metabolic rewiring in yeast cells. *Scientific Reports*, *8*, 13672. https://doi.org/10.1038/s41598-018-31939-9

Wang, Y., Eddy, J. A., & Price, N. D. (2012). Reconstruction of genome-scale metabolic models for 126 human tissues using mCADRE. *BMC Systems Biology*, *6*, 153. https://doi.org/10.1186/1752-0509-6-153

Wang, Y., Stancliffe, E., Fowle-Grider, R., Wang, R., Wang, C., Schwaiger-Haber, M., Shriver, L. P., & Patti, G. J. (2022). Saturation of the mitochondrial NADH shuttles drives aerobic glycolysis in proliferating cells. *Molecular Cell*, *82*, 3270–3283, e9. https://doi.org/10.1016/j.molcel.2022.07.007

Wintermute, E. H., Lieberman, T. D., & Silver, P. A. (2013). An objective function exploiting suboptimal solutions in metabolic networks. *BMC Systems Biology*, *7*, 98.

Yamauchi, Y., & Rogers, M. A. (2018). Sterol metabolism and transport in atherosclerosis and cancer. *Frontiers in Endocrinology*, *9*, 509. https://doi.org/10.3389/fendo.2018.00509

SUPPORTING INFORMATION

Additional supporting information can be found online in the Supporting Information section at the end of this article.

How to cite this article: Karabekmez, M. E. (2024). Insights into yeast response to chemotherapeutic agent through time series genome-scale metabolic models. *Biotechnology and Bioengineering*, *121*, 3351–3359. https://doi.org/10.1002/bit.28833